

# Preparation of Primary Amine Derivatives of the Magic-Size Nanocluster (CdSe)<sub>13</sub>

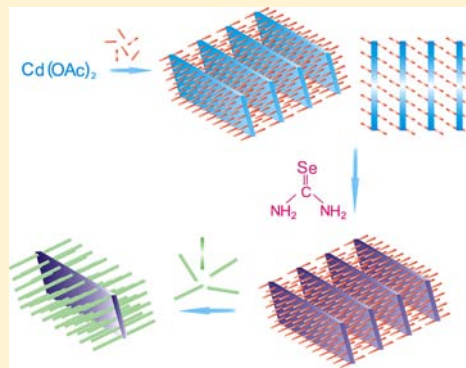
Yuanyuan Wang,<sup>†</sup> Yi-Hsin Liu,<sup>†</sup> Ying Zhang,<sup>†</sup> Paul J. Kowalski,<sup>‡</sup> Henry W. Rohrs,<sup>†</sup> and William E. Buhro<sup>\*,†</sup>

<sup>†</sup>Department of Chemistry, Washington University, St. Louis, Missouri 63130-4899, United States

<sup>‡</sup>Bruker Daltonics, Incorporated, 40 Manning Road, Billerica, Massachusetts 01821, United States

## Supporting Information

**ABSTRACT:** Four [(CdSe)<sub>13</sub>(RNH<sub>2</sub>)<sub>13</sub>] derivatives (R = *n*-propyl, *n*-pentyl, *n*-octyl, and oleyl) are prepared by reaction of Cd(OAc)<sub>2</sub>·2H<sub>2</sub>O and selenourea in the corresponding primary-amine solvent. Nanoclusters grow in spontaneously formed amine-bilayer templates and are characterized by elemental analysis, IR spectroscopy, UV–vis spectroscopy, TEM, and low-angle XRD. Derivative [(CdSe)<sub>13</sub>(*n*-propylamine)<sub>13</sub>] is isolated as a yellowish-white solid (MP 98 °C) on the gram scale. These compounds are the first derivatives of magic-size CdSe nanoclusters to be isolated in purity.



## INTRODUCTION

Discretely sized semiconductor nanoclusters have been spectroscopically detected since the early work of Henglein and co-workers<sup>1</sup> and observed as intermediates in the growth of larger colloidal nanocrystals.<sup>2–4</sup> Nanoclusters of CdSe have been of intense experimental<sup>5–8</sup> and theoretical<sup>9–11</sup> interest since their mass-spectrometric characterization by Kasuya and co-workers in 2004.<sup>12</sup> Among these so-called magic-size nanoclusters (CdSe)<sub>13</sub>, (CdSe)<sub>19</sub>, (CdSe)<sub>33</sub>, and (CdSe)<sub>34</sub> have been most studied. Until recently,<sup>13</sup> magic-size CdSe nanoclusters had been prepared only in mixtures of various sizes,<sup>5,8,14</sup> and no single, discrete-size nanocluster had been isolated in purity.

Our interest in magic-size CdSe nanoclusters began when we observed them as reaction intermediates in the low-temperature synthesis of wurtzitic CdSe nanoribbons or quantum belts.<sup>15,16</sup> In the course of our initial work, we isolated pure [(CdSe)<sub>13</sub>(*n*-octylamine)<sub>13</sub>] and [(CdSe)<sub>13</sub>(oleylamine)<sub>13</sub>].<sup>13</sup> As such compounds now appear to be useful nanocrystal synthons,<sup>15,16</sup> we sought to prepare a suitable derivative in gram quantities.

We now report full details of the synthesis and characterization of four primary amine derivatives of (CdSe)<sub>13</sub>, each having the stoichiometry [(CdSe)<sub>13</sub>(RNH<sub>2</sub>)<sub>13</sub>]. We show that each results from a templated synthesis in which the nanoclusters grow within amine-bilayer mesophases. The [(CdSe)<sub>13</sub>(*n*-propylamine)<sub>13</sub>] derivative is conveniently prepared on the gram scale. We hope that access to preparative quantities of (CdSe)<sub>13</sub> will promote further experimental studies of its structure, reactivity, physical properties, and use as a nanocrystal precursor.

## EXPERIMENTAL SECTION

**Materials.** *n*-Propylamine (+98%), *n*-pentylamine (+99%), *n*-octylamine (+99%), oleylamine (technical grade, 70%), Cd(OAc)<sub>2</sub>·2H<sub>2</sub>O, and trioctylphosphine (TOP, 97%) were purchased from Aldrich, and selenourea (99.9%, metal basis) was purchased from Alpha Aesar. All were used as received and stored under N<sub>2</sub>. Toluene from Sigma-Aldrich (CHROMASOLV, for HPLC, ≥99.9%) was purged with dry N<sub>2</sub> for at least 1 h and stored under N<sub>2</sub> prior to use.

**Analyses.** Elemental analyses (C, H, N) were obtained from Galbraith Laboratories, Inc. (Knoxville, TN). UV–vis spectra were obtained from a Perkin Lambda 950 UV/vis spectrometer. IR spectra were obtained from a Perkin-Elmer Spectrum BX FT-IR System. XRD patterns were obtained from a Rigaku Dmax A vertical powder diffractometer with Cu K $\alpha$  radiation ( $\lambda = 1.5418 \text{ \AA}$ ). Low-resolution TEM images were obtained from a JEOL 2000FX microscope operating at 200 KV. Melting point was obtained on a Mel-temp II Laboratory Device. Analysis by Rutherford backscattering spectrometry (RBS) was provided by the Characterization Facility at the University of Minnesota (Minneapolis, MN). LDI mass spectra were recorded on a Bruker ultrafleXtreme MALDI-TOF/TOF mass spectrometer. No matrix was employed in these mass-spectral analyses.

**Preparation of [(CdSe)<sub>13</sub>(*n*-propylamine)<sub>13</sub>].** All synthetic procedures were conducted under N<sub>2</sub>. In a large-scale synthesis, Cd(OAc)<sub>2</sub>·2H<sub>2</sub>O (1.30 g, 4.80 mmol) was dissolved in *n*-propylamine (40.0 g, 0.681 mol) in a septum-capped Schlenk tube, heated in a 50 °C oil bath for 1 h, and allowed to cool to room temperature. Selenourea (1.0 g, 8.2 mmol) was added in *n*-propylamine (10.0 g, 0.170 mol) in the glovebox and then sonicated in a benchtop sonicator for dissolution.

Received: October 23, 2012

Published: March 4, 2013



The selenourea solution was injected into cadmium-precursor solution at room temperature (20–25 °C) without stirring. The color of the reaction mixture changed immediately after injection from colorless (0 min) to light-yellow (viscous, 5 s), yellow (cloudy with a white precipitate, 1 min), and red (cloudy with a white precipitate, 1 h). After another 2 h under N<sub>2</sub> without stirring, (CdSe)<sub>13</sub> was deposited as reddish-white precipitate under a light-red supernatant.

The reaction mixture was subsequently heated at 50 °C in an oil bath for 40 min, during which the mixture turned a darker shade of red, with a white precipitate. The red solution contained elemental selenium as the colored byproduct, which was removed by addition of TOP (1.3 g) to form TOP = Se, resulting in a colorless solution with a white precipitate.

White precipitate was separated using a benchtop centrifuge (700 g, 30 s), and colorless supernatant was discarded. The remaining white slush was combined with a propylamine solution (20 mL, 20% w/w in toluene), and the mixture was recentrifuged and the supernatant discarded. This purification process was repeated 5 times in total. The residual solvent was removed in vacuo, leaving [(CdSe)<sub>13</sub>(*n*-propylamine)<sub>13</sub>] as a yellowish-white solid (1.19 g, 0.365 mmol, 97.5%).

Smaller-scale syntheses were conducted similarly, typically using Cd(OAc)<sub>2</sub>·2H<sub>2</sub>O (65 mg, 0.24 mmol) in *n*-propylamine (5.7 g, 0.097 mol) and selenourea (50 mg, 0.41 mmol) in *n*-propylamine (1.2 g, 9.3 mmol). The elemental-selenium byproduct was removed with added TOP (65 mg). Product precipitate was purified with a propylamine solution (5 × 5 mL, 20% w/w in toluene) as described above, leaving [(CdSe)<sub>13</sub>(*n*-propylamine)<sub>13</sub>] as a yellowish-white solid (59.3 mg, 0.018 mmol, 97.1%).

Characterization: MP (98 ± 2 °C). IR (KBr, cm<sup>-1</sup>, 25 °C): 3346 (w, NH stretch), 3245 (sh, NH stretch), 3202 (m), 3122 (m), 2953 (m), 2921 (s), 2869 (m), 2851 (m), 1646 (s, NH<sub>2</sub> deformation), 1559 (s, NH<sub>2</sub> deformation), 1458 (w), 1404 (s), 1351 (w), 1032 (w), 1007 (m), 965 (w) (Figure 1). UV–vis (toluene) λ<sub>max</sub> nm: 334, 349 (Figure

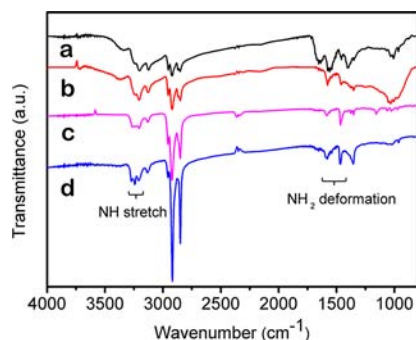


**Figure 1.** Infrared spectra (in KBr) of [(CdSe)<sub>13</sub>(RNH<sub>2</sub>)<sub>13</sub>] complexes; R = *n*-propyl (a), *n*-pentyl (b), *n*-octyl (c), and oleyl (d). All absorbances were assigned to the amine ligands. Regions characteristic for NH stretching and NH<sub>2</sub> deformation are identified.

2). Anal. Calcd for [(CdSe)<sub>13</sub>(*n*-propylamine)<sub>13</sub>]: C, 14.37; H, 3.59; N, 5.59. Found: C, 14.80; H, 3.46; N, 5.51. All values are given as percentages.

**Preparation of [(CdSe)<sub>13</sub>(*n*-pentylamine)<sub>13</sub>].** All synthetic procedures were conducted under the same general conditions for the [(CdSe)<sub>13</sub>(*n*-propylamine)<sub>13</sub>] preparation, except for the reaction solvent. Cd(OAc)<sub>2</sub>·2H<sub>2</sub>O (65 mg, 0.24 mmol) was dissolved in *n*-pentylamine (5.7 g, 0.066 mol), heated in a 70 °C oil bath for 1 h, and allowed to cool to room temperature. Selenourea (50 mg, 0.41 mmol) was dissolved in *n*-pentylamine (1.2 g, 0.013 mol).

After injecting the selenourea solution into the Cd(OAc)<sub>2</sub> solution at room temperature without stirring, the reaction mixture turned from colorless (0 min) to green yellow (1 min), light yellow (cloudy, 5 min), yellow (cloudy with a white precipitate, 15 min), and light red (cloudy with a white precipitate, 2 h). After another 5 h, a white precipitate formed under a red supernatant. The mixture was heated at 70 °C for 40 min. TOP (65 mg) was injected to remove the elemental-

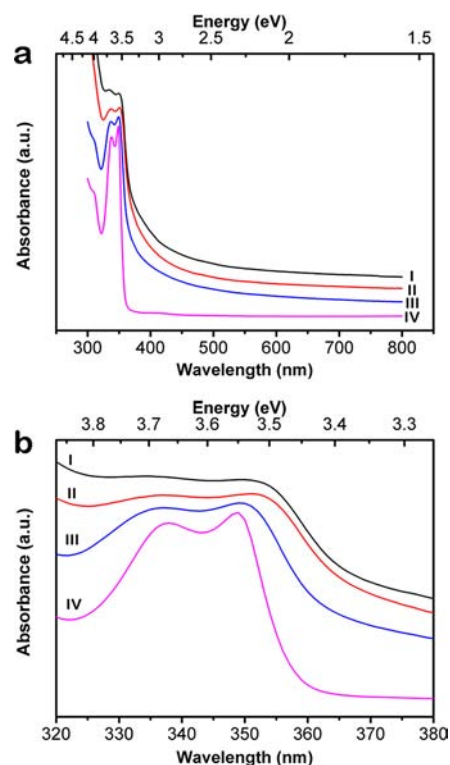


**Figure 2.** Absorption (extinction) spectra (in toluene dispersion) of [(CdSe)<sub>13</sub>(RNH<sub>2</sub>)<sub>13</sub>] complexes; R = *n*-propyl (I), *n*-pentyl (II), *n*-octyl (III), and oleyl (IV). (a) Full spectrum showing the characteristic absorbances of the (CdSe)<sub>13</sub> nanocluster. Note the scattering tails in spectra I–III. (b) Spectral expansions in the region of the characteristic absorptions near 337 and 349 nm (see text).

selenium byproduct. The remaining white precipitate was separated from the colorless supernatant using a purification process described above but with *n*-pentylamine solution (5 × 5 mL, 20% w/w in toluene). The residual solvent was removed in vacuo, leaving [(CdSe)<sub>13</sub>(*n*-pentylamine)<sub>13</sub>] as a slushy white solid (62.9 mg, 0.017 mmol, 92.6%). To ensure removal of the last traces of *n*-pentylamine for elemental analysis, pure toluene (5 × 5 mL) was used in the purification steps.

Characterization: IR (KBr, cm<sup>-1</sup>, 25 °C): 3368 (w, NH stretch), 3238 (sh, NH stretch), 3205 (m), 3128 (m), 2953 (w), 2920 (s), 2868 (sh), 2849 (s), 1577 (s, NH<sub>2</sub> deformation), 1458 (w), 1352 (w), 1031 (w), 1007 (w), 969 (w) (Figure 1). All values are given as percentages. UV–vis (toluene) λ<sub>max</sub> nm: 337, 351 (Figure 2). Anal. Calcd for [(CdSe)<sub>13</sub>(*n*-pentylamine)<sub>13</sub>]: C, 21.54; H, 4.67; N, 5.02. Found: C, 21.44; H, 4.42; N, 4.82.

**Preparation of [(CdSe)<sub>13</sub>(*n*-octylamine)<sub>13</sub>].** All synthetic procedures were conducted under the same general conditions for the [(CdSe)<sub>13</sub>(*n*-propylamine)<sub>13</sub>] synthesis, except for the reaction solvent. Cd(OAc)<sub>2</sub>·2H<sub>2</sub>O was dissolved in *n*-octylamine (5.7 g, 0.044 mol), heated in a 70 °C oil bath for 1 h, and allowed to cool to room temperature. Selenourea was dissolved in *n*-octylamine (1.2 g, 0.0093 mol).

After injecting selenourea solution into the Cd(OAc)<sub>2</sub> solution at room temperature, the reaction mixture turned from colorless (0 min) to green yellow (1 min), white yellow (cloudy, 5 min), yellow (cloudy, 15 min), and light red (cloudy, 2 h). After another 5–10 h, a white precipitate formed under a red supernatant. The reaction mixture was subsequently heated at 70 °C in an oil bath for 40 min. TOP (65 mg) was injected to remove elemental-selenium byproduct. The purification procedure was the same as that used in the synthesis [(CdSe)<sub>13</sub>(*n*-propylamine)<sub>13</sub>] but with *n*-octylamine solution (5 × 5 mL, 20% w/w in toluene). The residual solvent was removed in vacuo, leaving [(CdSe)<sub>13</sub>(*n*-octylamine)<sub>13</sub>] as a white slushy solid (75 mg,

0.018 mmol, 95.9%). To ensure removal of the last traces of *n*-octylamine for elemental analysis, pure toluene (5 × 5 mL) was used in the purification steps.

Characterization: IR (KBr, cm<sup>-1</sup>, 25 °C) 3260 (w, NH stretch), 3234 (w, NH stretch), 3204 (w), 2952 (m), 2922 (vs), 2850 (vs), 1584 (s, NH<sub>2</sub> deformation), 1466 (s), 1376 (w), 1352 (w), 1165 (w), 1062 (w), 1026 (w), 972 (w) (Figure 1). UV-vis (toluene) λ<sub>max</sub>, nm: 311, 337, 349 (Figure 2). MS *m/z* (relative intensity): 6507.5149 ((CdSe)<sub>34</sub>, 7.69%), 6318.0317 ((CdSe)<sub>33</sub>, 5.38%), 3638.1176 ((CdSe)<sub>19</sub>, 10.8%), 2488.5692 ((CdSe)<sub>13</sub>, 100%).<sup>13</sup> RBS: Cd:Se = 1.05:0.95.<sup>13</sup> Anal. Calcd for [(CdSe)<sub>13</sub>(*n*-octylamine)<sub>13</sub>]: C, 29.97; H, 5.97; N, 4.37. Found: C, 30.89; H, 5.84; N, 4.57.<sup>13</sup> All values are given as percentages.

**Preparation of [(CdSe)<sub>13</sub>(oleylamine)<sub>13</sub>].** All synthetic procedures were conducted under the same general conditions for the [(CdSe)<sub>13</sub>(*n*-propylamine)<sub>13</sub>] synthesis, except for the reaction solvent. Cd(OAc)<sub>2</sub>·2H<sub>2</sub>O was dissolved oleylamine (1.5 g, 5.6 mmol), heated in a 70 °C oil bath for 1 h, and allowed to cool to room temperature. Selenourea was dissolved in oleylamine (6.8 g, 0.025 mol). The color changes much slower after injecting selenourea solution into the Cd(OAc)<sub>2</sub> solution at room temperature. It changes from colorless (0 min) to bright green-yellow (transparent, 30 s), orange (viscous, overnight), and orange-red (cloudy, over 20 h). After 2 days, a white-orange precipitate formed under a red supernatant. TOP (65 mg) was injected to remove byproduct elemental-selenium. The purification procedure was the same as that used in the synthesis [(CdSe)<sub>13</sub>(*n*-propylamine)<sub>13</sub>] but with oleylamine solution (5 × 5 mL, 20% w/w in toluene). The residual solvent was removed in vacuo, leaving [(CdSe)<sub>13</sub>(oleylamine)<sub>13</sub>] as a white slushy solid (97 mg, 0.016 mmol, 86.6%). To ensure removal of the last traces of oleylamine for elemental analysis, pure toluene (5 × 5 mL) was used in the purification steps.

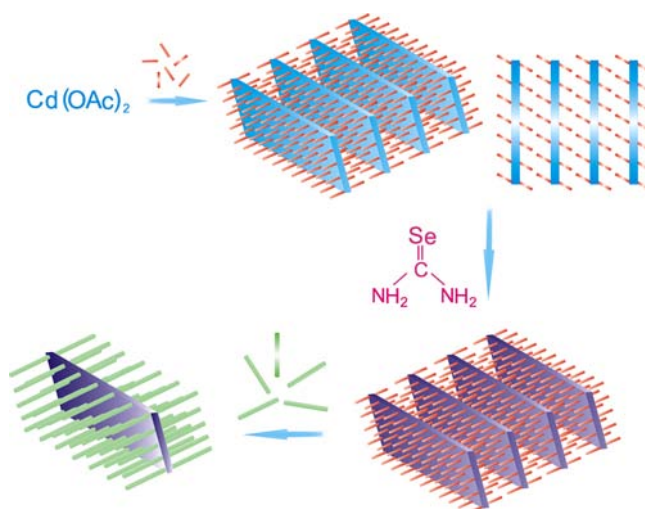
Characterization: IR (KBr, cm<sup>-1</sup>, 25 °C) 3271 (w, NH stretch), 3242 (m, NH stretch), 3208(m), 2955 (m), 2918 (vs), 2849 (vs), 1596 (sh, NH<sub>2</sub> deformation), 1578 (m, NH<sub>2</sub> deformation), 1466 (s), 1355 (s), 1018 (w), 963 (w) (Figure 1). UV-vis (toluene) λ<sub>max</sub>, nm: 310, 338, 349 (Figure 2). Anal. Calcd for [(CdSe)<sub>13</sub>(*n*-oleylamine)<sub>13</sub>]: C, 47.04; H, 8.06; N, 3.05. Found: C, 49.26; H, 8.84; N, 5.03. All values are given as percentages.

## RESULTS

We previously reported the room-temperature synthesis of [(CdSe)<sub>13</sub>(*n*-octylamine)<sub>13</sub>] by reaction of cadmium acetate (dihydrate) and selenourea in *n*-octylamine solvent.<sup>13</sup> Reaction monitoring established the chemical pathway summarized in Scheme 1. Combination of cadmium acetate and *n*-octylamine resulted in spontaneous formation of an amine-bilayer mesostructure<sup>17</sup> in which bilayers of *n*-octylamine separated cadmium acetate layers. This lamellar mesostructure served as a template for growth of (CdSe)<sub>13</sub> nanoclusters upon addition of selenourea. A mixture of magic-size CdSe nanoclusters was initially formed, including (CdSe)<sub>13</sub>, (CdSe)<sub>19</sub>, (CdSe)<sub>33</sub>, and (CdSe)<sub>34</sub>, which equilibrated exclusively to (CdSe)<sub>13</sub> over 5–7 h at room temperature.<sup>13</sup> We previously suggested that (CdSe)<sub>13</sub> is thermodynamically the most stable magic size within the amine-bilayer mesophase.<sup>13</sup>

A white slushy solid isolated from the equilibrated mixture was shown to be [(CdSe)<sub>13</sub>(*n*-octylamine)<sub>13</sub>] by a combination of elemental analysis, UV-vis spectroscopy, mass spectrometry, and Rutherford backscattering spectrometry (showing a Cd:Se ratio of 1:1).<sup>13</sup> Some have argued that mass-spectrometry evidence for magic-size-nanocluster mass distributions is questionable, because various specimens having apparently different distributions of magic-size nanoclusters appear to give very similar mass distributions.<sup>18</sup> However, our reported mass spectrum for (CdSe)<sub>13</sub> was markedly different than those published previously,<sup>12</sup> especially in that (CdSe)<sub>13</sub> was the base

## Scheme 1. Templated Chemical Pathway for Synthesis of [(CdSe)<sub>13</sub>(RNH<sub>2</sub>)<sub>13</sub>]<sup>13,15a</sup>



<sup>a</sup>Combination of Cd(OAc)<sub>2</sub> and the primary amine solvent forms a lamellar, bilayer template structure (blue, orange). Addition of selenourea results in growth of [(CdSe)<sub>13</sub>(RNH<sub>2</sub>)<sub>13</sub>] nanoclusters within the planar galleries of the template (purple, orange). Ligand exchange with oleylamine liberates sheet-like aggregates of [(CdSe)<sub>13</sub>(RNH<sub>2</sub>)<sub>13</sub>] (purple, green) from the bundled template.

peak, present in much greater intensity than the peaks for other (CdSe)<sub>x</sub> species.<sup>13</sup>

The template mesostructure remained intact in the as-synthesized [(CdSe)<sub>13</sub>(*n*-octylamine)<sub>13</sub>], with the (CdSe)<sub>13</sub> nanoclusters entrained within. We found that individual sheets of aggregated [(CdSe)<sub>13</sub>(*n*-octylamine)<sub>x</sub>(oleylamine)<sub>13-x</sub>] were exfoliated (Scheme 1) when the initially bundled template mesostructure was allowed to stand in oleylamine solution, during which partial ligand exchange occurred. Sonication of the sheet structures in oleylamine solution completed the ligand exchange, degraded the sheet aggregates, and released molecular [(CdSe)<sub>13</sub>(oleylamine)<sub>13</sub>] nanoclusters into solution.<sup>13</sup>

In this study, additional primary-amine derivatives of (CdSe)<sub>13</sub> were similarly prepared in the corresponding primary-amine solvent. [(CdSe)<sub>13</sub>(RNH<sub>2</sub>)<sub>13</sub>] nanoclusters were isolated as slushy solids except for [(CdSe)<sub>13</sub>(*n*-propylamine)<sub>13</sub>], which was a yellowish-white solid having a melting point of 98 °C. Satisfactory elemental analyses were obtained for [(CdSe)<sub>13</sub>(RNH<sub>2</sub>)<sub>13</sub>], R = *n*-propyl and *n*-pentyl. Elemental analysis for [(CdSe)<sub>13</sub>(*n*-octylamine)<sub>13</sub>] was slightly high in C, and that for [(CdSe)<sub>13</sub>(oleylamine)<sub>13</sub>] was significantly high in C, H, and N, reflecting our difficulty in successfully washing away the excess long-chain alkylamine (used as solvent) from these slushy solids. As expected, IR spectra of the [(CdSe)<sub>13</sub>(RNH<sub>2</sub>)<sub>13</sub>] compounds exhibited absorbances corresponding only to the primary amine ligands, with the characteristic NH stretches and NH<sub>2</sub> deformations<sup>19</sup> clearly observed (Figure 1). IR spectra of Cd(OAc)<sub>2</sub>·2H<sub>2</sub>O, *n*-octylamine, and [(CdSe)<sub>13</sub>(*n*-octylamine)<sub>13</sub>] are compared in Figure S1, Supporting Information, to establish that the observed absorbances of [(CdSe)<sub>13</sub>(*n*-octylamine)<sub>13</sub>] are displaced from those of the acetate ligand.

Evidence for the (CdSe)<sub>13</sub> stoichiometry of the as-synthesized nanoclusters was obtained by UV-vis spectroscopy (Figure 2). As we previously reported,<sup>13</sup> [(CdSe)<sub>13</sub>(*n*-octyl-

amine)<sub>13</sub>] exhibited three absorbances (311, 337, and 349 nm), which closely approached the electronic spectrum of (CdSe)<sub>13</sub> calculated theoretically (315, 330, and 345 nm).<sup>9</sup> Spectra of all four primary-amine derivatives were closely similar (Figure 2a), with small differences in peak positions and widths (Figure 2b) likely induced by the amine ligands. (The 315 nm absorbances were not resolved in the spectra of [(CdSe)<sub>13</sub>(*n*-propylamine)<sub>13</sub>] and [(CdSe)<sub>13</sub>(*n*-pentylamine)<sub>13</sub>].) Small variations in peak positions and line shapes in the absorption spectra of CdSe nanoclusters upon changes in surface ligation have been attributed to small perturbations of surface or electronic structure,<sup>20</sup> which seems to have occurred here as well.

Three of the Figure 2 spectra featured long scattering tails to longer wavelength, as a result of the bundled nature of the as-synthesized materials. This scattering tail was absent in the spectrum of [(CdSe)<sub>13</sub>(oleylamine)<sub>13</sub>], because exfoliation occurred readily upon solvent dispersion of this derivative for spectral analysis. Notably, absorbances at 363, 389, and 413 nm, previously assigned to (CdSe)<sub>19</sub>, (CdSe)<sub>33</sub>, and (CdSe)<sub>34</sub>,<sup>9,15</sup> were absent from all four spectra, establishing the spectroscopic purity of the [(CdSe)<sub>13</sub>(RNH<sub>2</sub>)<sub>13</sub>] nanoclusters.

The bundled and exfoliated template features were determined by TEM imaging (Figure 3). Figure 3a shows bundled aggregates of [(CdSe)<sub>13</sub>(*n*-octylamine)<sub>13</sub>].<sup>13,15</sup> Arrows

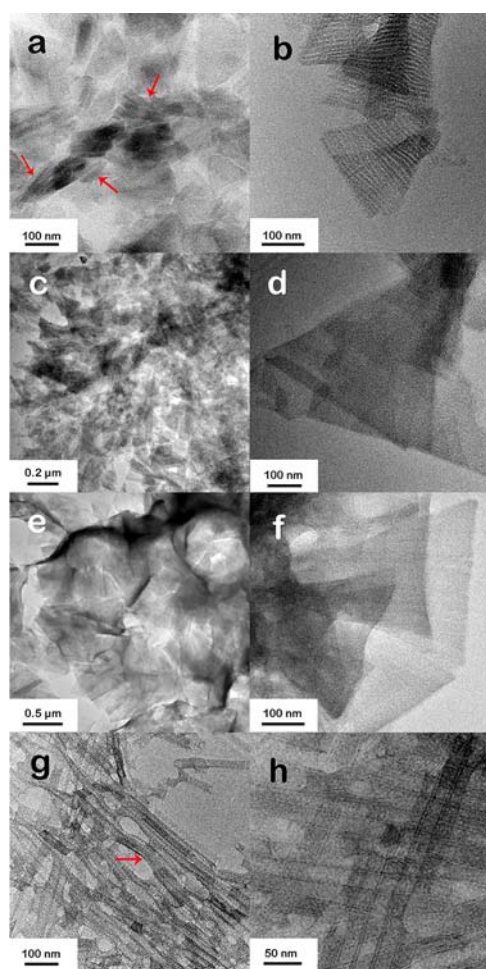


**Figure 3.** TEM images of the as-synthesized bundled (left column) and unbundled (right column) [(CdSe)<sub>13</sub>(RNH<sub>2</sub>)<sub>13</sub>]; R = *n*-octyl (a, b), *n*-propyl (c, d), *n*-pentyl (e, f), and oleyl (g, h). Arrows in parts a and g identify bundled regions.

indicate regions in which parallel stripes may be observed, constituting side views of the lamellar template depicted in Scheme 1. Exfoliation of individual layers from the lamellar mesophases as described above produced images like that in Figure 3b, in which triangular sheet-like aggregates of [(CdSe)<sub>13</sub>(*n*-octylamine)<sub>x</sub>(oleylamine)<sub>13-x</sub>] were separated from the bundled templates. The zebra-stripe pattern evident in Figure 3b revealed additional structural order within the individual sheets or layers.<sup>13,15</sup>

Images of the bundled and unbundled aggregates of [(CdSe)<sub>13</sub>(*n*-propylamine)<sub>13</sub>] and [(CdSe)<sub>13</sub>(*n*-pentylamine)<sub>13</sub>] are shown in Figure 3c–f. The lamellar-stripe pattern was not observed in the bundled aggregates of these compounds (Figure 3c and 3e), suggesting them to be less well ordered than the bundled aggregates of [(CdSe)<sub>13</sub>(*n*-octylamine)<sub>13</sub>] (Figure 3a). This observation was supported by low-angle XRD (see below). Exfoliation of these compounds produced individual triangular sheets, like those for [(CdSe)<sub>13</sub>(*n*-octylamine)<sub>13</sub>] (Figure 3b), confirming the initial lamellar architectures.

Images of “bundled” and unbundled aggregates of [(CdSe)<sub>13</sub>(oleylamine)<sub>13</sub>] (Figure 3g and 3h) contrasted with those of the other primary-amine derivatives. The most prominent feature in images of the as-synthesized [(CdSe)<sub>13</sub>(oleylamine)<sub>13</sub>] were rolled sheets resembling half-cylinders. Parallel-stripe patterns were observed in some regions of the images (see the arrow in Figure 3g), indicative of a bundled, lamellar architecture. We note that the bundled aggregates of [(CdSe)<sub>13</sub>(oleylamine)<sub>13</sub>] are the most easily exfoliated, as addition of oleylamine to the other bundled [(CdSe)<sub>13</sub>(RNH<sub>2</sub>)<sub>13</sub>] mesophases induces spontaneous exfoliation upon ligand exchange. We therefore surmise that solvent dispersion of the bundled [(CdSe)<sub>13</sub>(oleylamine)<sub>13</sub>] material for TEM sample preparation resulted in extensive exfoliation, as confirmed by the Figure 3h image. Low-angle XRD evidence is provided below for the bundled, lamellar structure of the as-synthesized material.

The low-angle XRD patterns (Figure 4) of the bundled [(CdSe)<sub>13</sub>(RNH<sub>2</sub>)<sub>13</sub>] mesophases provided strong confirma-

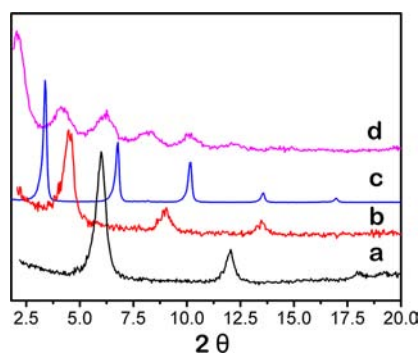


**Figure 4.** Low-angle XRD patterns of as-synthesized (bundled) [(CdSe)<sub>13</sub>(RNH<sub>2</sub>)<sub>13</sub>] showing the basal reflections produced by the lamellar mesostructures; R = *n*-propyl (a), *n*-pentyl (b), *n*-octyl (c), and oleyl (d).

tory evidence for their lamellar structures. Each contained a series of basal, 00*l*, reflections (Table 1) corresponding to the layered architectures. Peaks were sharpest for [(CdSe)<sub>13</sub>(*n*-octylamine)<sub>13</sub>], showing it to be the most highly ordered mesophase.

**Table 1. Experimental (Exp) and Calculated (Calcd) XRD Basal-Reflection Positions in  $[(\text{CdSe})_{13}(\text{RNH}_2)_{13}]$  Compounds**

$00l$	$[(\text{CdSe})_{13}(\text{oleylamine})_{13}]$ exp, deg, $2\theta$ (calcd, deg, $2\theta$ )	$[(\text{CdSe})_{13}(n\text{-octylamine})_{13}]$ exp, deg, $2\theta$ (calcd, deg, $2\theta$ )	$[(\text{CdSe})_{13}(n\text{-pentylamine})_{13}]$ exp, deg, $2\theta$ (calcd, deg, $2\theta$ )	$[(\text{CdSe})_{13}(n\text{-propylamine})_{13}]$ exp, deg, $2\theta$ (calcd, deg, $2\theta$ )
001	2.06	3.38	4.48	6.00
002	4.14 (4.12)	6.78 (6.76)	9.04 (8.96)	12.0 (12.0)
003	6.26 (6.18)	10.2 (10.1)	13.5 (13.4)	18.1 (18.0)
004	8.34 (8.24)	13.6 (13.5)		
005	10.2 (10.3)	17.0 (16.9)		
006	12.3 (12.4)			

The  $d$  spacings calculated from the XRD patterns gave the interlayer spacings in the four lamellar mesostructures, which are plotted versus the number of carbon atoms in the primary-amine ligands in Figure 5. Data gave the expected linear

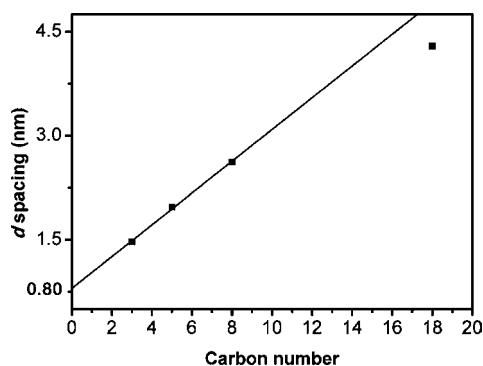


**Figure 5.** Plot of the measured basal-plane  $d$  spacing in the lamellar  $[(\text{CdSe})_{13}(\text{RNH}_2)_{13}]$  mesostructures obtained from the XRD data versus the number of carbon atoms in the primary-amine ligands.

relationship,<sup>21,22</sup> except for the oleylamine point, which departed from the line because of the double bond in the ligand's chain. The line should extrapolate approximately to the interamine-headgroup spacing at the  $y$  intercept, which was 0.80 nm. This value is close to the theoretical diameter of the  $(\text{CdSe})_{13}$  nanocluster (see the Discussion).<sup>10</sup> The result indicated that one monolayer of  $(\text{CdSe})_{13}$  nanoclusters was interspersed between the amine bilayers, represented as the planar features in Scheme 1, in the lamellar-template mesostructures.

## DISCUSSION

The results reported here establish that the four  $[(\text{CdSe})_{13}(\text{RNH}_2)_{13}]$  derivatives ( $R = n\text{-propyl}, n\text{-pentyl}, n\text{-octyl},$  and  $\text{oleyl}$ ) are accessible by a common synthetic method, are formed by a common templated-mesophase pathway, and possess a common stoichiometry. The solid derivative  $[(\text{CdSe})_{13}(n\text{-propylamine})_{13}]$  is readily prepared on the gram scale. Because  $[(\text{CdSe})_{13}(\text{RNH}_2)_{13}]$  compounds are useful low-temperature precursors to crystalline CdSe quantum belts<sup>15</sup> and presumably other CdSe nanocrystals and because ligand exchange in  $[(\text{CdSe})_{13}(\text{RNH}_2)_{13}]$  occurs readily, we expect that  $[(\text{CdSe})_{13}(n\text{-propylamine})_{13}]$  will prove to be a useful, isolable form of  $(\text{CdSe})_{13}$ .

Experimental structure determinations have not been completed for any magic-size CdSe nanocluster, including  $(\text{CdSe})_{13}$ . Indeed, no single- $x$ , magic-size  $(\text{CdSe})_x$  nanocluster had been isolated in purity until earlier this year.<sup>13</sup> However, the structure of  $(\text{CdSe})_{13}$  has been determined theoretically,<sup>9–12</sup> and the lowest energy  $C_3$  isomer found by Nguyen, Day, and Pachter is plotted in Figure 6.<sup>10</sup> These researchers

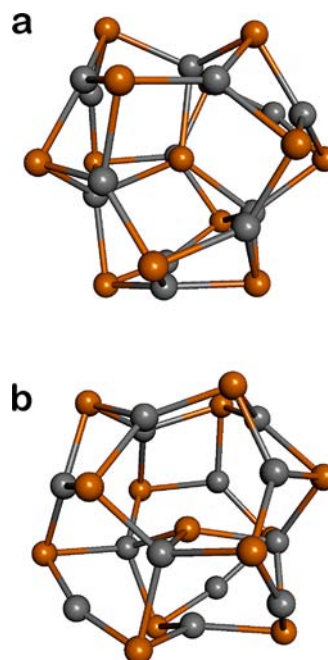


**Figure 6.** Two views of the lowest energy isomer of unligated  $(\text{CdSe})_{13}$  determined theoretically.<sup>6</sup> Cd atoms are gray, and Se atoms are orange. (a) View with the  $C_3$  axis perpendicular to the plane of the page; (b) view with the  $C_3$  axis oriented vertically in the plane of the page. Plots were made using Accelrys Discovery Studio Visualizer.

also found ligated nanoclusters of the type  $[(\text{CdSe})_x(n\text{-methylamine})_x]$  to be stable with one amine ligand datively bound to each Cd atom.<sup>10</sup> The structure of  $[(\text{CdSe})_{13}(n\text{-methylamine})_{13}]$  was not reported, the  $(\text{CdSe})_{13}$  component of which may differ from that in Figure 6. Calculations of the structural and spectral properties of  $[(\text{CdSe})_{13}(n\text{-methylamine})_{13}]$  are currently in progress.<sup>23</sup>

We measured the diameter of the  $(\text{CdSe})_{13}$  nanocluster in Figure 6 to be 0.78 nm using molecular-modeling software. This value is close to the interamine-headgroup spacing (0.80 nm) determined by analysis of the low-angle XRD data for the as-synthesized, bundled  $[(\text{CdSe})_{13}(\text{RNH}_2)_{13}]$  mesophases (see the Results section). The similarity of these values supports our claim that a single monolayer of  $(\text{CdSe})_{13}$  nanoclusters lies in each interamine-headgroup lamellar gallery.

The state of the magic-size CdSe nanocluster field may be compared to that of the carbon-fullerene field just prior to the reported isolation of  $C_{60}$  by Krätschmer and Huffman in 1990.<sup>24</sup> At that time,  $C_{60}$  had been characterized by mass spectrometry, its structure had been determined theoretically, and some of its spectroscopic properties were known. After pure  $C_{60}$  became available in gram quantities,<sup>24</sup> the carbon-fullerene field grew rapidly. Similarly, we propose that access to gram quantities of  $[(\text{CdSe})_{13}(n\text{-propylamine})_{13}]$  should enable

experimental structure determination, reactivity studies, and further determinations of the physical and spectroscopic properties of (CdSe)<sub>13</sub>.

## CONCLUSION

A convenient chemical synthesis affords the four [(CdSe)<sub>13</sub>(RNH<sub>2</sub>)<sub>13</sub>] derivatives (R = *n*-propyl, *n*-pentyl, *n*-octyl, and oleyl). These are the first derivatives of magic-size CdSe nanoclusters to be isolated in purity. The results establish the derivatives to have a common stoichiometry and to have formed by a common amine-bilayer-template pathway. Remarkably, even the shorter chain primary amines are able to generate amine-bilayer templates, which ultimately afford the [(CdSe)<sub>13</sub>(RNH<sub>2</sub>)<sub>13</sub>] products in mesophase architectures. Diffraction data collected from the [(CdSe)<sub>13</sub>(RNH<sub>2</sub>)<sub>13</sub>] mesophases allowed the first experimental estimate of the diameter of the (CdSe)<sub>13</sub> nanocluster (0.80 nm), which is close to the theoretical diameter. Access to gram quantities of (CdSe)<sub>13</sub> will enable further experimental studies.

## ASSOCIATED CONTENT

### Supporting Information

Figure providing an IR spectral comparison of Cd-(OAc)<sub>2</sub>·2H<sub>2</sub>O, *n*-octylamine, and [(CdSe)<sub>13</sub>(*n*-octylamine)<sub>13</sub>]. This material is available free of charge via the Internet at <http://pubs.acs.org>.

## AUTHOR INFORMATION

### Corresponding Author

\*E-mail: [buhro@wustl.edu](mailto:buhro@wustl.edu).

### Notes

The authors declare no competing financial interest.

## ACKNOWLEDGMENTS

This work was supported by the NSF under grant CHE-1012898 (to W.E.B.) and grants from the National Center for Research Resources (5P41RR000954-35) and the National Institute of General Medical Sciences (8 P41 GM103422-35) from the National Institutes of Health (to H.W.R.). We thank Ruth Pachter and Kiet A. Nguyen (Air Force Research Laboratory, Wright-Patterson Air Force Base, Dayton, OH) for providing the coordinates of (CdSe)<sub>13</sub> and sharing information prior to publication. We also thank Fudong Wang (Washington University) for helpful discussions.

## REFERENCES

- (1) Fojtik, A.; Weller, H.; Koch, U.; Henglein, A. *Ber. Bunsen Ges. Phys. Chem.* **1984**, *88*, 969.
- (2) Peng, Z. A.; Peng, X. G. *J. Am. Chem. Soc.* **2002**, *124*, 3343.
- (3) Soloviev, V. N.; Eichhofer, A.; Fenske, D.; Banin, U. *J. Am. Chem. Soc.* **2001**, *123*, 2354.
- (4) Cumberland, S. L.; Hanif, K. M.; Javier, A.; Khitrov, G. A.; Strouse, G. F.; Woessner, M.; Yun, C. S. *Chem. Mater.* **2002**, *14*, 1576.
- (5) Cossairt, M.; Owen, J. S. *Chem. Mater.* **2011**, *23*, 3114.
- (6) Kudera, S.; Zanella, M.; Giannini, C.; Rizzo, A.; Li, Y. Q.; Gigli, G.; Cingolani, R.; Ciccarella, G.; Spahl, W.; Parak, W. J.; Manna, L. *Adv. Mater.* **2006**, *19*, 548.
- (7) Kui, Y. *Adv. Mater.* **2012**, *24*, 1123.
- (8) Noda, Y.; Maekawa, H.; Kasuya, A. *Eur. Phys. J. D* **2010**, *57*, 43.
- (9) Ben, M. D.; Havenith, R. W. A.; Broer, R.; Stener, M. *J. Phys. Chem. C* **2011**, *115*, 16782.
- (10) Nguyem, K. A.; Day, P. N.; Pachter, R. *J. Phys. Chem. C* **2010**, *114*.

- (11) Singh, T.; Mountziaris, T. J.; Maroudas, D. *Appl. Phys. Lett.* **2012**, *100*, 053105.
- (12) Kasuya, A.; Sivamohan, R.; Barnakov, Y. A.; Dmitruk, I. M.; Nirasawa, T.; Romanyuk, V. R.; Kumar, V.; Mamykin, S. V.; Tohji, K.; Jeyadevan, B.; Shinoda, K.; Kudo, T.; Terasaki, O.; Liu, Z.; Belosludov, R. V.; Sundararajan, V.; Kawazoe, Y. *Nat. Mater.* **2004**, *3*, 99.
- (13) Wang, Y. Y.; Liu, Y. H.; Zhang, Y.; Wang, F. D.; Kowalski, P. J.; Rohrs, H. W.; Loomis, R. A.; Gross, M. L.; Buhro, W. E. *Angew. Chem., Int. Ed.* **2012**, *51*, 6154.
- (14) Dukes, A. D., III; McBride, J. R.; Rosenthal, S. J. *Chem. Mater.* **2010**, *22*, 6402.
- (15) Liu, Y. H.; Wang, F. D.; Wang, Y. Y.; Gibbons, P. C.; Buhro, W. E. *J. Am. Chem. Soc.* **2011**, *133*, 17005.
- (16) Liu, Y. H.; Wayman, V. L.; Gibbons, P. C.; Loomis, R. A.; Buhro, W. E. *Nano Lett.* **2010**, *10*, 352.
- (17) Yener, D. O.; Sindel, J.; Randall, C. A.; Adair, J. H. *Langmuir* **2002**, *18*, 8692.
- (18) Evans, C. M.; Love, A. M.; Weiss, E. A. *J. Am. Chem. Soc.* **2012**, *134*, 17298.
- (19) Lambert, J. B.; Shurvell, H. F.; Verbit, L.; Cooks, R. G.; Stout, G. H. In *Organic Structural Analysis*; Macmillan Publishing Co., Inc.: New York, 1976.
- (20) Cossairt, B. M.; Juhas, P.; Billinge, S. L.; Owen, J. S. *J. Phys. Chem. Lett.* **2011**, *2*, 3075.
- (21) Ikawa, N.; O., Y.; Kimura, T. *J. Mater. Sci.* **2008**, *43*, 4198.
- (22) Kitaigorodsky, A. I. *Molecular crystals and molecules*; Academic Press: New York, 1973.
- (23) Pachter, R.; Nguyen, K. A. *Personal communication*.
- (24) Krätschmer, W.; Lamb, L. D.; Fostiropoulos, K.; Huffman, D. R. *Nature* **1990**, *347*, 354.